ELSEVIER

Journal of Chromatography A, 967 (2002) 279–287

JOURNAL OF CHROMATOGRAPHY A

www.elsevier.com/locate/chroma

Theory for the capillary electrophoretic separation of DNA in polymer solutions

Ho Jin Jung, Young Chan Bae*

Division of Chemical Engineering and Molecular Thermodynamics Lab., Hanyang University, Seoul 133-791, South Korea

Received 14 November 2001; received in revised form 2 May 2002; accepted 3 June 2002

Abstract

We present a mathematical model based on the models of Hubert et al. [Macromolecules 29 (1996) 1006] and Sunada and Blanch [Electrophoresis, 19 (1998) 3128] to describe the electrophoretic mobility of DNA by a transient entanglement coupling mechanism. The proposed model takes into account the interactions between molecules in the capillary and the cross-section of collision between DNA and polymer molecules. The results show that the calculated values agree remarkably well with our electrophoretic mobility data.

Keywords: Mathematical modelling; DNA; Polymers

1. Introduction

Electrophoresis has proved a very efficient technique for the separation of DNA. For the past several decades, slab gel electrophoresis has been widely used to separate DNA, however it has the disadvantages of a large thermal gradient, band broadening, and the time consumed by gel loading. Compared with conventional gel electrophoresis, capillary electrophoresis (CE) is a powerful technique for the separation of DNA due to high efficiencies and speed [1–3]. Recently, uncrosslinked polymer solutions have been used as a sieving medium, because crosslinked polymer gel-filled capillaries are unstable under the condition of high electric fields [4–8].

In 1991, Soane and co-workers [9,10] proposed that the mechanism of separation was the same in gels and polymer solutions, asserting that ‘‘pores’’ are formed in entangled polymer solutions that lead to the separation of DNA either by the Ogston sieving or reptation mechanisms. Viovy and Duke [11] modified the biased reptation model to represent the dynamic nature of the uncrosslinked polymer solutions by a process termed ‘‘constraint release’’. The mechanism of the model is that the polymer molecules making up the ‘‘tube’’ through which the DNA is reptating, are themselves allowed to reptate through the solution so that the tube dimensions fluctuate with the movement of the polymer molecules. Barron et al. [6] have proposed a transient entanglement coupling mechanism for the separation of DNA in polymer solutions, the only current mechanism that can explain separations in dilute polymer solutions. The transient entanglement coupling mechanism asserts that DNA collides with

*Corresponding author. Tel.: +82-22-290-0529; fax: +82-22-296-6280.

E-mail address: ycbae@hanyang.ac.kr (Y.C. Bae).

0021-9673/02/$ – see front matter
PII: S0021-9673(02)00743-4

polymer molecules and is forced to drag the polymer through the solution, thus increasing the frictional force acting on the DNA and reducing its electrophoretic mobility. Note that the mechanism is not solely restricted to dilute solutions; the mechanism may apply to both dilute and entangled polymer solutions. Indeed, the character of the DNA separation does not change in the transition from a dilute to an entangled polymer solution: similar separations are obtained in a range of concentrations around entanglement threshold concentration with no apparent shift in the behaviour of DNA [6,8]. Hubert et al. [12] developed a mathematical model based on this early interpretation of transient entanglement coupling and compared the model with the data for hydroxyethylcellulose (HEC) polymer solution (M_r = 24 000–27 000) reported by Barron et al. [6]. They described a separation mechanism whereby when DNA and polymer collide, they entangle and both the DNA and the polymer slide around each other and then release. Thus they use the mean lifetime of DNA–polymer contact to consider the effect of the interaction between the polymer molecule and DNA.

In 1998, Sunada and Blanch [13] modified the transient entanglement coupling mechanism to incorporate nonentangling collision during DNA separations in solutions of low-molecular-mass polymers and compared with the experimental data for several concentrations of hydroxyethylcellulose (M_r = 139 000 g/mol) and hydroxypropylcellulose (M_r = 100 000 g/mol). The model, however, ignored the specific interactions between DNA and polymer molecules, such as hydrogen bonding. Thus the collision model could not be applied to the DNA separation in entangled solution of high-molecular-mass polymers.

In this study, we present a mathematical model based on the models of Hubert et al. and Sunada and Blanch to describe the transient entanglement coupling mechanism. We compare our proposed model with our experimental data.

2. Experimental

2.1. Materials

ΦX174-Hae III restriction digest (11 fragments) was purchased from Sigma (St. Louis, MO, USA) at a concentration of 606 μg/ml. The DNA digest was diluted to 100 μg/ml with distilled and deionised (DI) water. Benzyl alcohol was used as a neutral marker to measure electroosmotic flow (Aldrich, Milwaukee, WI, USA). Tris(hydroxymethyl)-aminomethane (Tris) was from Sigma. Ethylenediaminetetraacetic acid (EDTA) and boric acid were from Aldrich. The buffer used in this experiment was 89 m*M* Tris, 89 m*M* boric acid, and 5 m*M* EDTA (TBE buffer), which naturally reaches a pH of 8.3. HEC with average molecular masses of 90 000, 250 000, 720 000 and 1 300 000 g/mol were from Aldrich. A measured amount of HEC was added to the buffer solution at room temperature under mechanical stirring for 24 h to obtain a homogeneous polymer solution. Chlorotrimethylsilane, diethylamine and glass distilled ether were purchased from Aldrich. Celite 545, filter agent, was from Shinyo (Osaka, Japan).

2.2. Diethylaminotrimethylsilane synthesis

The diethylaminotrimethylsilane synthesis was modified from diamino monomers synthesis [14]. Chlorotrimethylsilane (5 ml) and diethylamine (3 ml) were added to anhydrous ether (100 ml) and reacted with stirring in an ice bath for 2 h. The reaction is shown in Fig. 1. The solution of product was filtered using celite 545-packing column to remove salts and a solution of diethylaminotrimethylsilane in ether, was then obtained.

2.3. Capillary preparation

In all experiments, 31.2 cm (effective length 21 cm)×75 μm I.D., fused-silica capillaries (Beckman Instruments, Fullerton, CA, USA) were used. Untreated fused-silica capillaries were pretreated by rinsing 1.0 *M* NaOH solution for 30 min and then with DI water for 30 min. Residual water was evaporated from the capillaries at 100 °C. In the process of coating, the capillary was first flushed with ether for 20 min and then was flushed with the solution of diethylaminotrimethylsilane in ether under nitrogen for 1 h. Next the capillary was flushed with nitrogen gas and rinsed with 1 *M* HCl solution. The reaction mechanism is shown in Fig. 1.

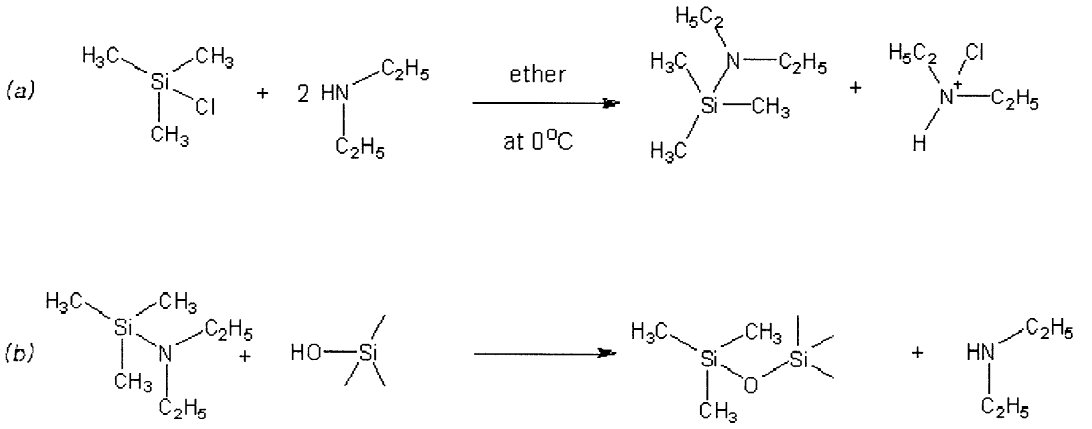

Fig. 1. Schematic representations of (a) the synthesis of diethylaminotrimethylsilane and (b) the silanisation with diethylaminotrimethylsilane.

2.4. Capillary electrophoresis

A Beckman P/ACE system MDQ (Beckman Instruments, Fullerton, CA, USA) was used for CE analysis. Instrument control and data collection were performed using an IBM 586 computer utilising P/ACE system MDQ program. CE separations were performed using 31.2 cm (21 cm to the window)×75 μm capillaries. The coated capillary for DNA analysis was first rinsed with DI water for 5 min and then rinsed with TBE buffer for 5 min. Next the coated capillary was rinsed with HEC solution for 5–10 min according to its viscosity. The DNA digest sample was introduced into the capillary by electromigration at 3 kV for 2 s (96.154 V/cm). The electrophoresis was carried out under negative polarity at 25 °C. An ultraviolet detector was used with the filter set at 254 nm.

3. Theoretical consideration

This theory is based on the principle that polymer molecules in solution impart a drag force on DNA molecules during a transient entanglement coupling [13]. We introduce the mean lifetime of DNA–polymer contact [12] to the theory. We develop this model with two assumptions, similar to Sunada and Blanch's model. The model assumes the polymer sample is monodisperse, which we know to be inaccurate. The HEC 139 K sample has a polydispersity (M_w/M_n) of over five, as the number-average molecular mass (M_n) is between 24 000 and 27 000 g/mol. This implies that the majority of the polymer molecules in the solution have a relatively small molecular mass, close to M_n, but the presence of a smaller number of average molecular mass, M_w. Unfortunately, the distribution of molecular masses in the sample is not known, so we are not able to compensate for the polydispersity in our model, and we are forced to rely on the weight-average molecular mass (M_w) for our predictions. In order to test the effects of polymer polydispersity, it would be useful to examine separations employing a low-molecular-mass, monodisperse polymer. The model also assumes a uniform distribution of the spatial location of polymer molecules in solution. The drag force on the DNA without contact with polymer molecules and the drag force imparted by the polymer obstacle during transient entanglement coupling with DNA counterbalance the electrophoretic force acting on the DNA molecule:

$$F_e = F_{DNA} + F_p \quad (1)$$

where F_{DNA} is the drag force on the DNA without contact with polymer molecules, and F_p is the drag force imparted by the polymer obstacle during transient entanglement coupling with DNA.

The electrophoretic force, F_e, has been defined as:

$$F_e = q_{eff} N_{DNA} E \quad (2)$$

where q_{eff} is the effective charge per base pair, N_{DNA} is the number of base pairs of the DNA molecule, and E is the electric field strength. The effective charge per base pair has been estimated to be $0.066-0.1e$ per base pair [15,16] in a buffered solution. In the model calculations, we use a value of $0.1e$.

The drag force on the DNA without contact with polymer molecules, F_{DNA}, acts in the direction of its motion and is given by:

$$F_{DNA} = f_{DNA} N_{DNA} v \quad (3)$$

where v is the velocity of the DNA and f_{DNA} is its translational friction coefficient per base pair in polymer solution, which is affected by the concentration of polymer and polymer molecular mass which determine the effect of the shear stress; the smaller blob size [17] of polymer solution, the stronger shear stress results. We assumed that DNA's translational friction coefficient per base pair in polymer solution depends only on the molecular mass of polymer since the slight changes of polymer concentration have a little influence on blob size shown by Eq. (4). Thus we use the mean value of f_{DNA} for various concentration of polymer with different molecular masses.

$$\xi_b = 1.43 R_g (C/C^*)^{-3/4} \quad (4)$$

where ξ_b is the blob size of polymer solution, R_p is the radius of gyration of the polymer, C is the polymer concentration and C^* is the entanglement threshold concentration. The drag force due to the polymer molecules is given by:

$$F_p = f_p v p \quad (5)$$

where p is the number of polymer molecules dragged by DNA and f_p is the friction coefficient of the polymer, which is given as below for a non-free-draining random coil

$$f_p = \frac{4\pi^2 \eta R_p}{3} \quad (6)$$

where η is the solvent viscosity and R_p is the radius of gyration of the polymer as given [17]:

$$R_p \cong \left(\frac{K M_r^{(1+d)}}{6.2 N_A} \right)^{1/3} \quad (7)$$

Table 1
Molecular parameters of different polymers used in capillary electrophoresis[a]

Polymer	K (ml/g)	d
Polyacrylamide	$6.31 \cdot 10^{-3}$	0.8
Hydroxypropylcellulose	$6.31 \cdot 10^{-3}$	0.8
Polyethyleneoxide	$1.25 \cdot 10^{-2}$	0.78
Hydroxyethylcellulose	$9.53 \cdot 10^{-3}$	0.87
Methylcellulose	$3.16 \cdot 10^{-1}$	0.55
Dextran	$4.93 \cdot 10^{-2}$	0.60

[a] The K and d values are taken from Ref. [18].

where d and K are characteristic constants for a given polymer–solvent system (see Table 1), M_r is the molecular mass of the polymer and N_A is Avogadro's number. Thus, at steady state, the effective mobility of the DNA dragging one or more polymer molecules is

$$\mu_p = \frac{q_{eff} N_{DNA} E}{f_{DNA} N_{DNA} + f_p p} \quad (8)$$

X is the average number of polymers dragged by the DNA, so it could be less than unity. Imagine that one DNA has a polymer attached for only half the time it spends in the capillary. The time it takes to exit the capillary will be given by the mobility with one DNA attached for 50% of the time, together with its mobility with no DNA attached for 50% of the time. For this reason we introduce P to account for the case of $X<1$. If $X>1$, then the mobility is averaged over the number of polymers attached.

The average number of polymer molecules dragged by a DNA, X, is given by:

$$X = \frac{\tau_{eff} N_C \bar{\mu} E}{L_d} \quad (9)$$

where N_C is the number of DNA–polymer collisions that occur during the electrophoresis and $\bar{\mu}$ is the average electrophoretic mobility during the electrophoresis. The parameter, τ_{eff}, is the effective time constant of the DNA–polymer contact [12]. This parameter is proportional to the DNA size since the probability of DNA–polymer contact increases with DNA size.

$$\tau_{eff} = \chi_{eff} N_{DNA} \quad (10)$$

where χ_{eff} is the effective time constant per base

pair. We assumed from observation of experimental data that χ_{eff} has the relation of the function of polymer concentration. For HEC, χ_{eff} is inversely proportional to the polymer concentration since as the polymer solution is concentrated, the increase of the interaction between the oxygen atom of HEC and the hydroxyl group of HEC and the decrease of the interaction between the oxygen atom of DNA and the hydroxyl group of HEC result in the decrease of χ_{eff}.

$$\chi_{\text{eff}}(C) = a + bC \tag{11}$$

where C is the concentration of polymer solution. Thus τ_{eff} is given by:

$$\tau_{\text{eff}} = (a + bC)\, N_{\text{DNA}} \tag{12}$$

Combining Eqs. (9) and (12) X is given by:

$$X = \frac{(a + bC)N_{\text{DNA}}N_{\text{C}}\bar{\mu}E}{L_{\text{d}}} \tag{13}$$

The number of DNA–polymer collisions, N_{C}, is calculated from a collision theory analogy:

$$N_{\text{C}} = \frac{CN_{\text{A}}}{M_{\text{r}}} \cdot \pi(R_{\text{DNA}} + R_{\text{p}})^2 L_{\text{d}} \tag{14}$$

where $\pi(R_{\text{DNA}} + R_{\text{p}})^2$ is the collision cross-sectional area. The radius of gyration of the DNA molecule, R_{DNA}, is calculated by the Porod–Kratky equation:

$$R_{\text{DNA}} = \left[\frac{1}{3} \cdot L_{\text{C}}L_{\text{p}} - L_{\text{p}}^2 + \frac{2L_{\text{p}}^3}{L_{\text{C}}} - \frac{2L_{\text{p}}^4}{L_{\text{C}}^2}\left(1 - \text{e}^{-\frac{L_{\text{C}}}{L_{\text{p}}}}\right) \right]^{1/2} \tag{15}$$

where L_{C} is the contour length of the DNA and L_{p} is the persistence length of the DNA. We calculate R_{DNA} using a value of 450 Å for L_{p}. The average effective mobility of the DNA, $\bar{\mu}$, will be given by:

$$\bar{\mu} = (X - P)\mu_{P+1} + (P + 1 - X)\mu_P \tag{16}$$

where P is an integer value such that $P < X < P + 1$. Combining Eqs. (13) and (16) and rearranging for $\bar{\mu}$, the average effective mobility is given by:

$$\bar{\mu} = \frac{(P + 1)\mu_P - P\mu_{P+1}}{\left[1 + \dfrac{(a + bC)N_{\text{DNA}}N_{\text{C}}E}{L_{\text{d}}} \cdot (\mu_P - \mu_{P+1})\right]} \tag{17}$$

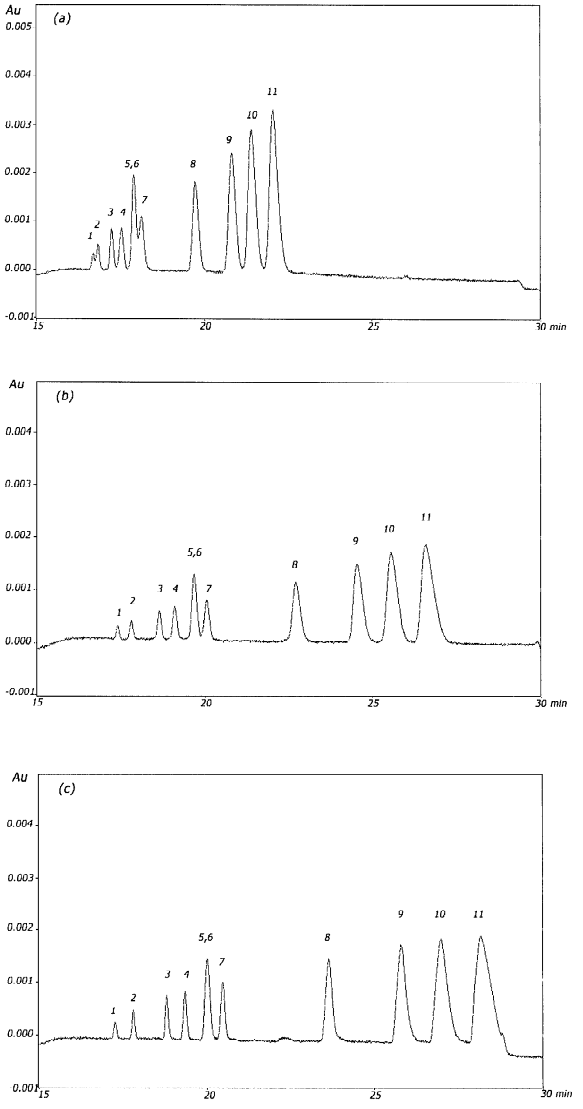

Fig. 2. Electrophoretic separation of ΦX174-Hae III restriction digest using M_{r} 250 000 HEC for each concentration (a) 0.245% (w/v), (b) 0.4% (w/v), (c) 0.5% (w/v). Conditions: 2 kV applied voltage (64.103 V/cm), negative polarity; UV detection at 254 nm; electrokinetic injection at 3 kV (96.154 V/cm) for 2 s. Peaks: 1=72, 2=118, 3=194, 4=234, 5=271, 6=281, 7=310, 8=603, 9=872, 10=1078 and 11=1353 bp.

4. Results and discussion

Our model clearly shows that the separations of DNA in low-molecular-mass polymer solutions can be explained by nonentangling collisions between DNA and polymer molecules. Additionally, the model is able to explain separations in dilute polymer solutions, whereas the Ogston and reptation models fail.

As we compare the models of Hubert et al. with that of Sunada and Blanch, on which our model is based, there are both similarities and differences. The basis for both models is that hydrodynamic drag forces resulting from DNA–polymer collisions results in a reduction of mobility of the DNA and leads to separation of DNA. However, the mechanism of separation is completely different in the two models. The Hubert et al. model assumes that when DNA and polymer collide, they entangle and both the DNA and the polymer slide around each other and release. The model we present assumes that when DNA and polymer collide, they do not entangle, but the polymer molecule imparts a hydrodynamic drag force upon the DNA.

Despite the vastly different mechanisms upon which the models are based, they share the common assumption that separation of DNA results from hydrodynamic drag forces imparted upon the DNA by polymer molecules. This is where the two models converge (to a point). Despite these similarities, there are significant differences in the approaches of the authors. Huber et al. rely on scaling arguments to derive a final equation that contains two adjustable parameters, γ and β. Our model is based on molecular parameter wherever possible, whereas Hubert et al. scale these parameters. Additionally, Hubert et al. use the entire experimental data set to fit two parameters (γ and β) and then compare their model predictions using these parameters. The predictive ability of the model is thus not examined. The model presented by Sunada and Blanch has only one adjustable parameter, the product of τ_c and λ_{eff}, and they calculate this value using only the electrophoretic data from one concentration in a data set,

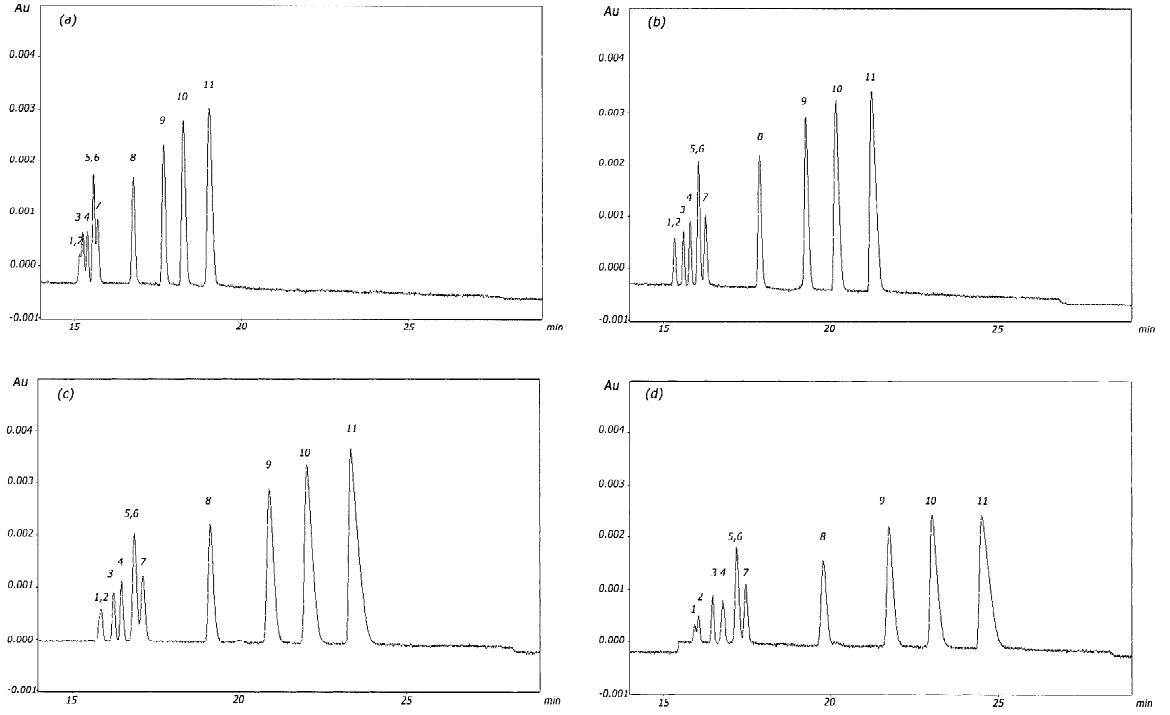

Fig. 3. Electrophoretic separation of ΦX174-Hae III restriction digest using M_r 720 000 HEC for each concentration (a) 0.1% (w/v), (b) 0.15% (w/v), (c) 0.18% (w/v), (d) 0.2% (w/v) All other conditions as in Fig. 1.

and predict the rest of the data set using this value. In this sense, Sunada and Blanch's model is predictive, while the Hubert et al. model only provides a fit of two parameters to a data set.

The model of Hubert et al. appears to be slightly more accurate in predicting the mobilities, especially at higher concentrations. Both models are less accurate at predicting the behaviour of DNA smaller than 200 base pairs (bp). Although Hubert et al. state that the ''collision process itself might be different'' than their proposed mechanism for larger polymer, videomicroscopic evidence clearly shows that U-shape collisions and ''brief'' collisions are ubiquitous in solution containing large polymers.

The difference between Sunada and Blanch's model and our model is that whereas they used one adjustable parameter, the product of τ_c and λ_{eff}, we used two adjustable parameters, a and b, to calculate the electrophoretic mobility. Therefore, they could not consider the effect of the concentration of the polymer solution. The one adjustable parameter they used, $\tau_c \lambda_{eff}$, is a constant. Instead, we used two adjustable parameters, a and b, to calculate $a + bC$, which is a function of the polymer solution concentration. Therefore, we can say that our model is more accurate.

We have compared the proposed model with the experimental data for HEC polymer ($M_r = 250\,000$, 720 000 and 1 300 000 g/mol) solutions in Figs. 2–4. These experiments were performed with negative polarity, using a very stable capillary coated with trimethylchlorosilane that can minimise the electroosmotic flow (EOF). The parameters f_{DNA} and χ_{eff} are determined from Eq. (17), using the electrophoretic mobilities of DNA fragments at various concentrations of polymer solution with each different molecular mass (Table 2).

The parameter f_{DNA} decreases with increasing the polymer molecular mass since the increase of blob size with polymer molecular mass results in the decrease of shear stress on DNA.

The effective time constant per base pair decreases

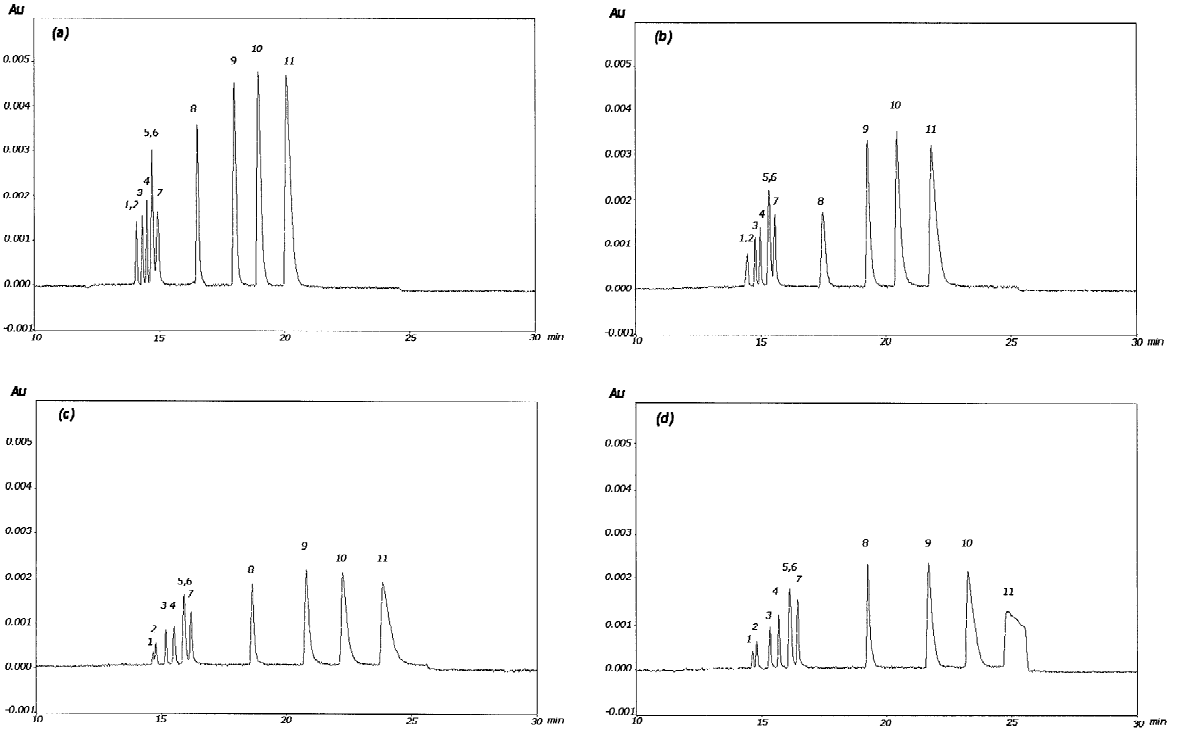

Fig. 4. Electrophoretic separation of ΦX174-Hae III restriction digest using M_r $1.3 \cdot 10^6$ HEC for each concentration (a) 0.12% (w/v), (b) 0.15% (w/v), (c) 0.18% (w/v), (d) 0.2% (w/v) All other conditions as in Fig. 1.

Table 2
List of the model parameters, f_{DNA} and χ_{eff}

Molecular mass (g/mol)	f_{DNA} (g/s bp)	Function of χ_{eff} (s/bp)
250 000	2.806^{-8}	1.05308^{-6}–2.94808^{-5} C
720 000	2.502^{-8}	1.41238^{-6}–6.16443^{-5} C
1 300 000	2.072^{-8}	1.33321^{-6}–5.98612^{-5} C

linearly with the increasing of polymer concentration in entanglement region. The trend of decreasing χ_{eff} results from the increase in the interaction between the oxygen atom of HEC and the hydroxyl group of HEC and the decrease of the interaction between the oxygen atom of DNA and the hydroxyl group of HEC.

We have compared the model with experimental data of HEC (M_r = 250 000, 720 000 and 1 300 000 g/mol) solutions with various concentrations in Fig. 5. The shape of the mobility curve is well represented, with the exception of the range of small DNA (<200 bp). It is quite likely that for DNA smaller than 200 bp, the radius of gyration calculated by the Porod–Kratky equation is no longer valid as the DNA will be acting more like a rod in solution than a random coil. Thus we compare the theory with the mobilities of DNA that can be applied by the Porod–Kratky equation. The model predicts both the steeper slope for small DNA fragments and the plateau in mobility as the DNA size increase. The model also provides excellent predictions of the effect of increasing concentration and polymer molecular mass on the mobility of DNA.

Our model clearly shows that the separations of DNA in entangled high-molecular-mass polymer solutions can be explained by a transient entanglement coupling mechanism between DNA and polymer molecules.

5. Conclusion

We present a model which takes into account the interactions between molecules and the cross-section of collision between DNA and polymer molecules. Our model shows a good agreement with experimental data. It clearly describes the separation of DNA by a transient entanglement coupling mechanism.

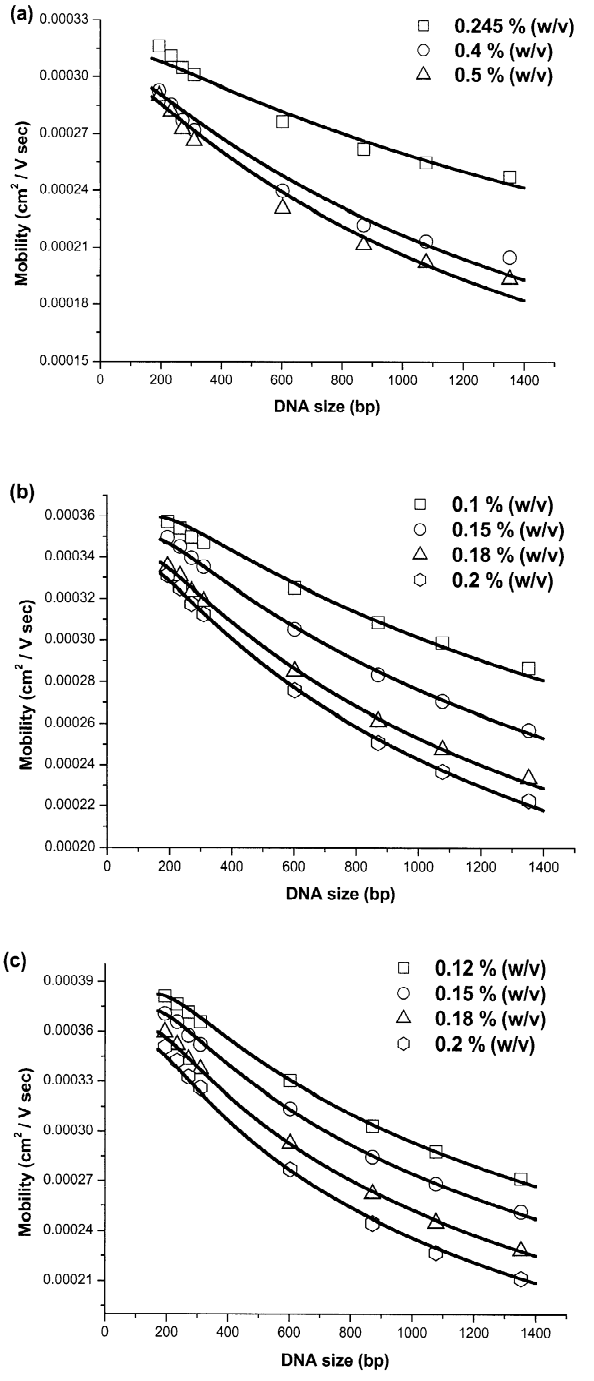

Fig. 5. Comparison of the calculated electrophoretic mobilities with experimental data for (a) M_r 250 000 HEC solutions, (b) M_r 720 000 HEC solutions, (c) M_r $1.3 \cdot 10^6$ HEC solutions. The solid lines are calculated by this work. The symbols represent experimental data. The model parameters, f_{DNA} and χ_{eff} are listed in Table 2.

Thus our model represents well the DNA separation in entangled high-molecular-mass polymer solutions.

Acknowledgements

The International Cooperation in Korea Science and Engineering Foundation supported this article.

References

[1] A.S. Cohen, D. Najarian, J.A. Smith, B.L. Karger, J. Chromatogr. 458 (1988) 323.
[2] C. Heller, J. Chromatogr. A 698 (1995) 19.
[3] P. Camilleri, Capillary Electrophoresis: Theory and Practice, CRC Press, Boca Raton, FL, 1997.
[4] E.A. Ribeiro, J. Chromatogr. 618 (1993) 181.
[5] C. Getfi, A. Orsi, P.G. Righetti, V. Brancolini, L. Cremonesi, M. Ferrari, Electrophoresis 15 (1994) 640.
[6] A.E. Barron, H.W. Blanch, D.S. Soane, Electrophoresis 15 (1994) 597.
[7] A.E. Barron, W.M. Sunada, H.W. Blanch, Electrophoresis 15 (1995) 64.
[8] A.E. Barron, W.M. Sunada, H.W. Blanch, Electrophoresis 17 (1996) 744.
[9] P.D. Grossman, D.S. Soane, Biopolymers 31 (1991) 1221.
[10] Y.C. Bae, D.S. Soane, J. Chromatogr. A 652 (1993) 17.
[11] J.-L. Viovy, T. Duke, Electrophoresis 14 (1993) 322.
[12] S.J. Hubert, G.W. Slater, J.-L. Viovy, Macromolecules 29 (1996) 1006.
[13] W.M. Sunada, H.W. Blanch, Electrophoresis 19 (1998) 3128.
[14] C. Wang, C. Zhang, S.M. Lee, R.L. Dalton, Macromolecules 34 (2001) 2359.
[15] S.B. Smith, A.J. Bendich, Biopolymers 29 (1990) 1167.
[16] J.M. Schurr, S.B. Smith, Biopolymers 29 (1990) 1161.
[17] C. Heller, Electrophoresis 19 (1998) 1691.
[18] M. Kurata, Y. Tsunashima, in: J. Brandrup, E.H. Immergut (Eds.), Polymer Handbook, Wiley, New York, 1989, p. 1, Chapter 7.